2011年 8月
박사학위논문

Gadoxetic acid uptake of hepatocellular carcinoma: Correlation with pathologic features and molecular transporters

조선대학교 대학원
의 학 과
최 수 진

Gadoxetic acid uptake of hepatocellular carcinoma: Correlation with pathologic features and molecular transporters

간세포암의 gadoxetic acid 섭취: 조직학적 성상과 분자 운반체와의 상관관계

2011 年 8 月 25 日

조선대학교 대학원

의 학 과

최 수 진

Gadoxetic acid uptake of hepatocellular carcinoma: Correlation with pathologic features and molecular transporters

지도교수 전 제 열

이 논문을 의학박사학위 논문으로 제출함

2011 年 4 月 日

조선대학교 대학원

의 학 과

최 수 진

최수진의 의학박사학위논문을 인준함

위원장	조선대학교 교수	염철호	인
위 원	조선대학교 교수	김도경	인
위 원	전남대학교 교수	정용연	인
위 원	조선대학교 교수	최 석	인
위 원	조선대학교 교수	전제열	인

2011 年 6 月 日

조선대학교 대학원

CONTENTS

CONTENTS OF FIGURES

국문초록

간세포암의 gadoxetic acid 섭취: 조직학적 성상과 분자 운반체와의 상관관계

최 수 진

지도교수: 전 제 열
조선대학교 대학원 의학과

목적: 간세포암의 Gadoxetic acid의 간담도기 조영증강 자기공명영상(MRI)의 조영증강 양상과 조직학적 성상 및 담즙 생성과의 연관성 및 섭취 기전을 알아보고자 하였다.

대상과 방법: MRI를 시행하고 수술로 확진 된 40예의 간세포암을 대상으로 하였다. Gadoxetic acid 주입전과 주입 후 20분 간담도기 MRI를 지방억제 T1 강조 경사에코를 이용하여 얻었다. MRI에서 주변 간 실질의 신호강도에 대한 종괴의 신호강도비를 계산하여 종양의 상대적 조영증강비 (relative enhancement ratio; RER)를 구하였다. 조직병리학적 성상들은 Edmondson-Steiner grading 에 따라 종양의 분화도(I-IV)와 종양의 증식성(지주성, 가성선형, 치밀형)으로 관찰하였고, 종괴의 피막존재여부와 종양 내

담즙의 생성 정도 3단계(경증, 중등도, 중증)로 분류하였다. 면역조직학적 분석은 종양의 OATP8과 MRP2의 발현 정도를 3단계로 분류하여 조직병리학적 성상들과 MRI에서 상대적 조영증강비와 연관성 유무를 분석하였다.

결과: 종양의 평균 RER은 0.65±0.11이었고, 종양분화도 등급 I, II, III의 상대적 조영증강비는 각각 0.72±0.11, 0.63±0.23, 그리고 0.68±0.10이였으며 통계적 유의성은 없었다(P=0.32). 종양의 증식형태에 따른 RER은 지주성 은 0.69±0.12, 가성선형 0.62±0.01 그리고 치밀형 0.62±0.09 이었으며 통계적 유의성은 없었다(P=0.26). 담즙생성 정도에 따른 RER은 경증 0.64±0.01, 중등도 0.70±0.11, 중증 0.68±0.10로 통계적 의의를 보이지 않았다(P=0.43). 종양 내 OATP8 및 MRP2의 발현정도는 각각 1.54와 2.71이었으며 각각의 correlation coefficient (r)는 0.055 (P=0.735)와 - 0.325 (P=0.038)이었고, MRP2의 발현정도가 종양 내부에서 의미 있게 증가하였다.

결론: 간담도기 조영증강 MRI에서 Gadoxetic acid의 섭취는 종양의 분화도나 증식형태 혹은 담즙생성과는 큰 연관성이 없고, OATP8의 발현정도 보다는 종양 내 MRP2의 발현 증가가 간세포암의 조영증강에 영향을 준다.

I. INTRODUCTION

Gadoxetic acid is a recently developed hepatocyte-selective contrast agent for magnetic resonance (MR) imaging (1-3). This contrast agent combines the properties of a conventional extracellular fluid contrast agent and a hepatocyte-specific agent. As a result of these properties, gadoxetic acid provides a delayed hepatobiliary imaging as well as a dynamic perfusion imaging. Gadoxetic acid is taken up approximately 50% of the administered dose by hepatocytes and cleared from the body into bile and urine (4-5). This rate of the hepatocyte uptake is much higher than the hepatic uptake of another liver-specific contrast agent, gadobenate dimeglumine, approximately 5% of the injected dose. It allows maximal enhancement of diffusely damaged as well as normal liver parenchyma on delayed hepatobiliary imaging at about 20 minutes after injection of gadoxetic acid, which thus improves the detection and characterization of malignant hepatic lesions including hepatocellular carcinoma (HCC) (6). Some studies proved that gadoxetic acid-enhanced MR imaging is superior to standard MR imaging using gadolinium chelates or spiral CT in the diagnosis of focal liver lesions that lack functioning hepatocytes (7-11). Gadoxetic acid-enhanced MR imaging, especially

including hepatobiliary phase images improved diagnosis of HCC and assisted in surgical planning (12).

It has been known that organic anion transporting polypeptides (OATPs) are sodium-independent organic anion transporters that are expressed in many tissues of the human, including the liver, kidney, intestine and brain. OAPTs transport various endogenous and xenobiotic organic anion substances into the human hepatocytes. Gadoxetic acid is also an organic anion (1-3). Therefore it enters into normal hepatocytes through OATPs, especially OATP1B1, OATP8 (OATP1B3), and NTCP (Na_/taurocholate cotransporting polypeptide) expressed at the basolateral membrane, and comes out in bile mediated by the canalicular transporter, multidrug resistance-associated protein 2 (MRP2) and MRP3 expressed on the sinusoidal side of hepatocytes (13, 14). Gadoxetic acid enhancement of the healthy hepatic parenchyma may be influenced by the expression degree of OATPs and MRP2 at hepatocytes. Consequently, enhancement of HCCs on gadoxetic acid MR imaging also seems to correlate with expression of these import and export transporters within the tumor cell.

Although several reports showed that isointensity or hyperintensity of HCC on hepatobiliary phase MR image may be correlated with expression level of OATP8 as well as MRP3,

and with bile accumulation of bile in the tumors and degree of histological differentiation (15-19), the mechanism of uptake and excretion of gadoxetic acid in human hepatocytes and hepatic tumors still have not been well investigated. Further evaluation is needed to confirm the mechanism of gadoxetic acid enhancement at hepatic parenchyma and HCCs.

The purpose of this study is to correlate the enhancement of HCCs with histopathologic features and molecular transporters, and to evaluate the mechanism of gadoxetic acid uptake of HCCs on hepatobiliary phase of gadoxetic acid-enhanced MR imaging.

II. METHODS

Patients

This retrospective study was approved from our institutional review board, and informed consent requirement for this study was waived by our institutional review board. Between Jun 2009 and Jan 2010, 288 consecutive patients, suspected of having HCC underwent gadoxetic acid-enhanced MR imaging with the hepatobiliary phase at 20 minutes. Exclusion data were 248 patients, including 201 patients who took preoperative treatments, such as transcatheter arterial chemoembolization, percutaneous ethanol injection therapy or radiofrequency ablation, 29 patients who had less than 1cm or over than 5cm sized HCC, 15 patients who underwent MR imaging with inadequate imaging sequences, 2 patients who had hemosiderosis or hemochromatosis, and one patient who did not have pathological diagnosis specifically because of massive tumor necrosis. Finally, forty of 40 patients with HCC were included, and the total number of including HCC nodules was 40. The diagnosis of HCC was based on surgical resection in all 40 patients. Mean size of the resected tumor was 2.93cm (range, 1.20-4.30cm).

Mean patient age was 52 years for the entire study group

(range, 40-81 years). Thirty-three were men (range, 40-74 years; mean, 55 years) and seven were women (range, 42-81 years; mean, 46 years). Twenty-nine patients had underlying hepatic cirrhosis caused by hepatitis B virus (HBV) in 27 patients and hepatitis C virus (HCV) in one patient. One patient had alcoholic liver cirrhosis. Eleven patients had a normal liver including ten hepatitis B carriers. One patient had no underlying hepatic problem. In these patients, hepatic function was estimated according to the Child-Pugh classification. 36 patients had class A liver cirrhosis and 4 patients was included in class B (Table 1).

Gadoxetic Acid-enhanced MR Imaging

Gadoxetic acid-enhanced MR imaging was taken within one month (mean, 13.5 days; range, 1-28 days) before surgical resection. MRI examinations were performed with a 3.0T MR scanner (Magnetom Tim trio, Siemens, Germany) with a 12-channel phased-array coil as the receiver coil in all patients. The MRI protocols and sequences were as follows: a fat-suppressed T1-weighted gradient-echo in-phase sequence (TR/TE: 111.0 ms/2.5 ms, flip angle: 70.0°, matrix: 320 × 154, bandwidth: Hz per pixel), an out-of-phase sequence (TR/TE:

111.0 ms/6.2 ms, flip angle: 70.0°, matrix: 320 × 154, bandwidth: Hz per pixel), a respiratory-triggered single-shot T2-weighted sequence with a reduction factor of two or four (TR/TE: 2,000 ms/180 ms, flip angle: 150°, matrix: 320 × 230, bandwidth: Hz per pixel), a respiratory-triggered single-shot heavily T2-weighted sequence with a reduction factor of two or four (TR/TE: 5,153 ms/81 ms, flip angle: 140°, matrix: 320 × 230, bandwidth: Hz per pixel) with a 5-7 mm section thickness, a 1-mm to 2-mm intersection gap and a field of view of 360x260 mm. A dose of 0.1 mL/kg (0.025 mmol/kg gadoxetic acid) contrast agent was automatically administered intravenously at a rate of 2 mL/sec, followed by a 20 mL saline solution flush. For the contrast-enhanced MR imaging, the unenhanced, arterial phase (20 sec), portal phase (60 sec), equilibrium phase (3 min), and hepatobiliary phase sequences (20 min) sequences were obtained using a fat-suppressed T1-weighted gradient-echo in-phase sequence (TR/TE: 3.5 ms/1.3 ms, flip angle: 9°, matrix: 320 × 154, bandwidth: Hz per pixel) with a 3 mm section thickness with no intersection gap and a field of view of 360x260 mm.

Analysis of MR Images

For quantitative analysis of signal intensities (SIs) of the tumor and adjacent background hepatic parenchyma, the regions of interest (ROI) was used at pre-contrast and post-contrast hepatobiliary phase MR images. The ROI of the tumor was taken as one maximum oval or round area at the level of the largest diameter of the mass devoid of necrotic area. Three ROIs for measurement of SIs of the non-tumorous region were set over the surrounding background hepatic parenchyma, avoiding large vascular structures. These ROIs were round areas up to 10mm in diameter. The mean value of three ROIs was used as the SI of adjacent background hepatic parenchyma. The relative intensity ratio (RIR) of the tumor to the adjacent hepatic parenchyma on pre-contrast and post-contrast MR images was calculated with the formulas, RIR = $SI_{tumor}/SI_{liver.}$ To assess real enhancement of the tumor, there relative enhancement ratio (RER) of the tumor, which means the enhancement of tumors compared with that of the adjacent hepatic parenchyma, was calculated according to the following formula: RER = RIR_{post}/RIR_{pre}, where RIR_{post} is the post-contrast relative intensity ratio and RIR_{pre} is the pre-contrast relative intensity ratio (20).

Analysis of Histopathologic Features

Hematoxylin-eosin (HE) staining of the tissue was performed for all 40 resected liver specimens, and then the tumor differentiation was classified into four grades according to Edmondson-Steiner grading (21, 22). The proliferative pattern of HCCs was classified into trabecular, pseudoglandular and compact pattern and was analyzed whether the tumor capsule was present or not. The degree of bile production was rated by % of bile accumulation in the tumor which represents greenish colored bile pigment inside the pseudo-cholangiole, bile canaliculi, or cytoplasm of the tumor cells. The bile production was stratified into three-point scale; mild (<5%), moderate (5-25%), severe (>25%). The RER of HCC was correlated with regard to histopathologic features including tumor differentiation, proliferative pattern and the degree of bile production.

Analysis of Immunohistochemical Features

Immunohistochemical staining of tumors and the adjacent hepatic parenchyma was preformed with a staining kit (Vecta stain ABC Peroxidase, Burlingame, Calif) for OATP8 and MRP2.

Thereafter, the expression degree of OATP8 and MRP2 of the tumor was evaluated by using following three-point scale: score 0, negative or minimal; score 1+, positive to the same or lesser extent compared with the adjacent parenchyma; and score 2+, positive to a higher degree than the adjacent liver parenchyma. Immunopositivity was determined by staining of the membrane or hepatocystes or tumor cells by no in terms of cytoplasmic reactivity, if present.

Statistical Analysis

Statistical significance was analyzed with SPSS software (SPSS, version 11.0, Chicago, IL, USA). The one-way ANOVA test was used for the analysis of the tumor enhancement and tumor differentiation, proliferation pattern of the tumor and the degree of tumor bile production. Then the Pearson correlation test was used to evaluate the relationship between the tumor enhancement ratio and the expression degree of OATP8 and MRP2, with a correlation coefficient (r) of $\geq$ 0.8 indicating strong correlation. A P value of less than 0.05 was considered to indicate a statistically significant difference.

III. RESULTS

Correlation with Enhancement Ratio on MR Imaging and Histopathologic Features:

Post-contrast RSI of HCC was lower than that of pre-contrast RSI. The mean RER for all HCCs was 0.65±0.11 (Figure 1). Of the 40 HCCs, 21 (52.5%) were in Edmondson-Steiner grade III, 16 (40.0%) were grade II, 2 (0.05%) and 1 (0.025%) were grade I and IV, respectively. The RER of grade I was higher than that of others (Figure 2). However, there was no significantly difference in the pre- and post-contrast RSI to histological differentiation (P=0.32).

The RERs of HCCs with trabecular (n=30), pseudoglandular (n=2), and compact (n=8) pattern were 0.69±0.12, 0.62±0.01, and 0.62±0.09, respectively (Figure 3). There was no significantly difference in RER to proliferative pattern of the tumor (P=0.26) (Figure 4).

The RERs of HCCs with mild (n=25), moderate (n=10), and severe (n=2) bile production were 0.64±0.01, 0.70±0.11, and 0.68±0.10, respectively. The RER was not significantly correlated with the degree of bile production (P=0.43) (Figure 5).

The RERs of HCCs with capsule (n=26) and without capsule (n=14) were 0.67±0.12 and 0.64±0.08, respectively (P=0.28).

Expression Degree of OATP8 and MRP2:

The mean expression degree of OATP8 was 1.537 in all HCCs. However, the OATP8 activity of surrounding liver parenchyma was 2.707. The RER ratio was not significantly correlation with the expression degree of OATP8 in the tumor (correlation coefficient r=0.055, $P \geq 0.05$).

The mean expression degree of MRP2 was 2.707 in all HCCs and the MRP2 activity of surrounding liver parenchyma was 2.024. The RER was strong negatively correlated to the expression degree of MRP2 in the tumor (correlation coefficient r=-0.325,$P \leq 0.05$) (Figure 6 & 7).

Table 1. Clinical Features of Including Patients

No. of Patients (n=40)	
Age (Y: year)	Mean 52Y (range; 40-81Y)
Male-to-female ratio	33 : 7
Tumor size (cm)	2.93 (range, 1.20-4.30cm)
Child-Pugh classification (n=40)	
Class A	36
Class B	4
Hepatic cirrhosis (n=29)	
HBV	27
HCV	1
Alcoholic	1
Normal liver parenchyma (n=11)	
Chronic hepatitis B carrier	10
No underlying disease	1

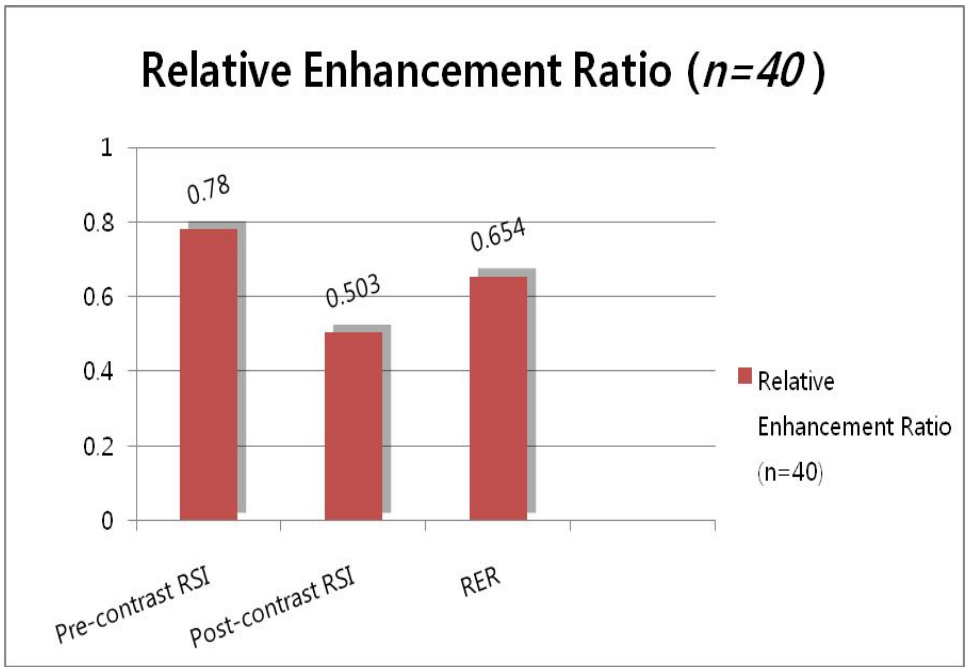

Figure 1. The graphs demonstrating pre- and post-relative signal intensities and relative enhancement ratio in all HCCs.

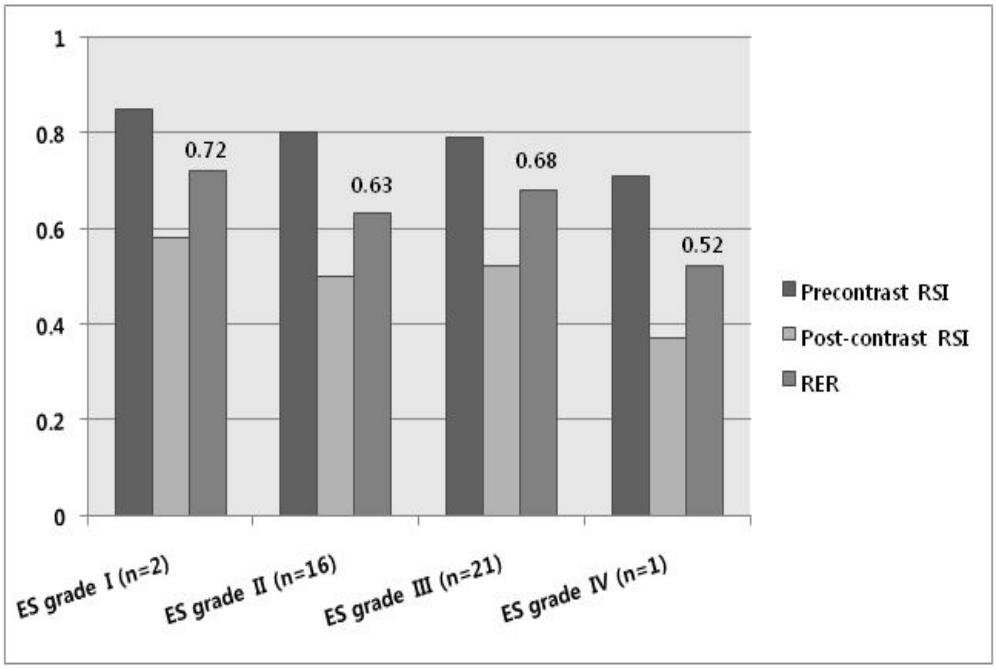

Figure 2. The graphs illustrating pre- and post-relative signal intensities (RSI) and relative enhancement ratio (RER) according to tumor differentiation. The post RSI and PER of grade II HCCs have lower than those of the grade III HCC.

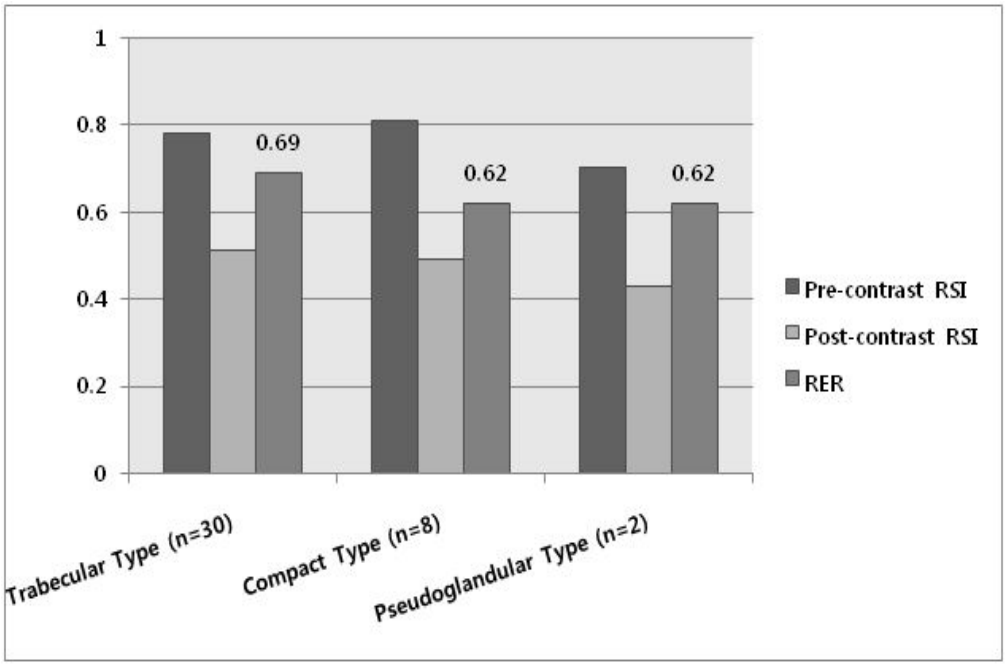

Figure 3. The graphs illustrating pre- and post-relative signal intensities (RSI) and relative enhancement ratio (RER) according to tumor proliferating pattern. The pre-RSI of HCC with compact type has higher than those of other two HCCs. The RER of HCCs is not statistically significant.

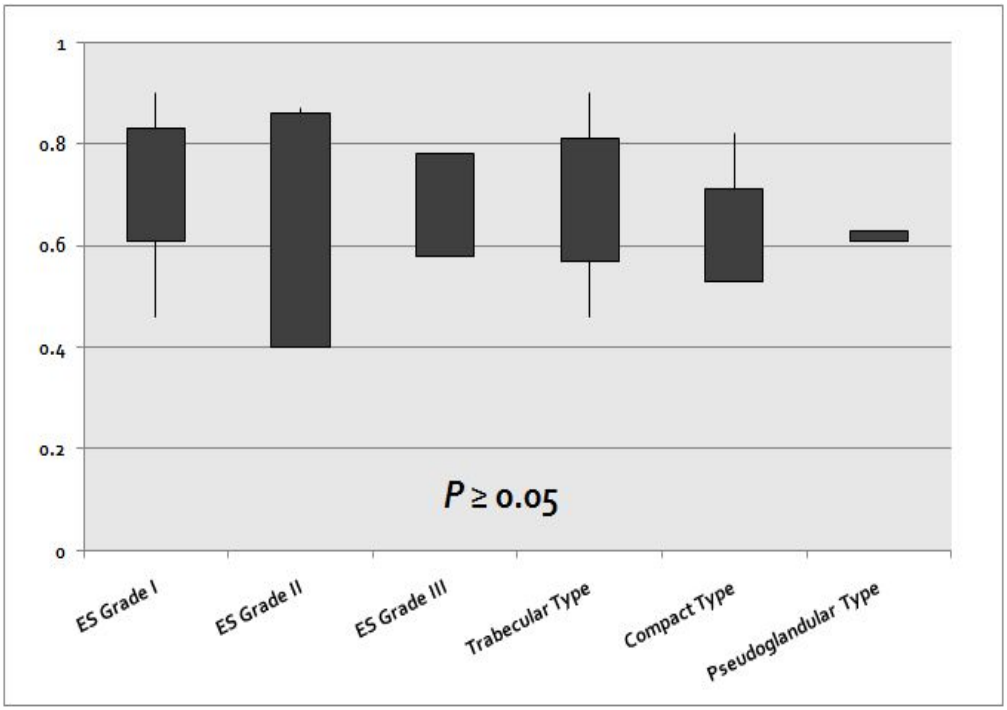

Figure 4. Box plots of relative enhancement ratio (RER) of HCCs according to histopathologic features. There is no significantly difference in RER to histological differentiation (P=0.32) nor to proliferative pattern of the tumor (P=0.26)

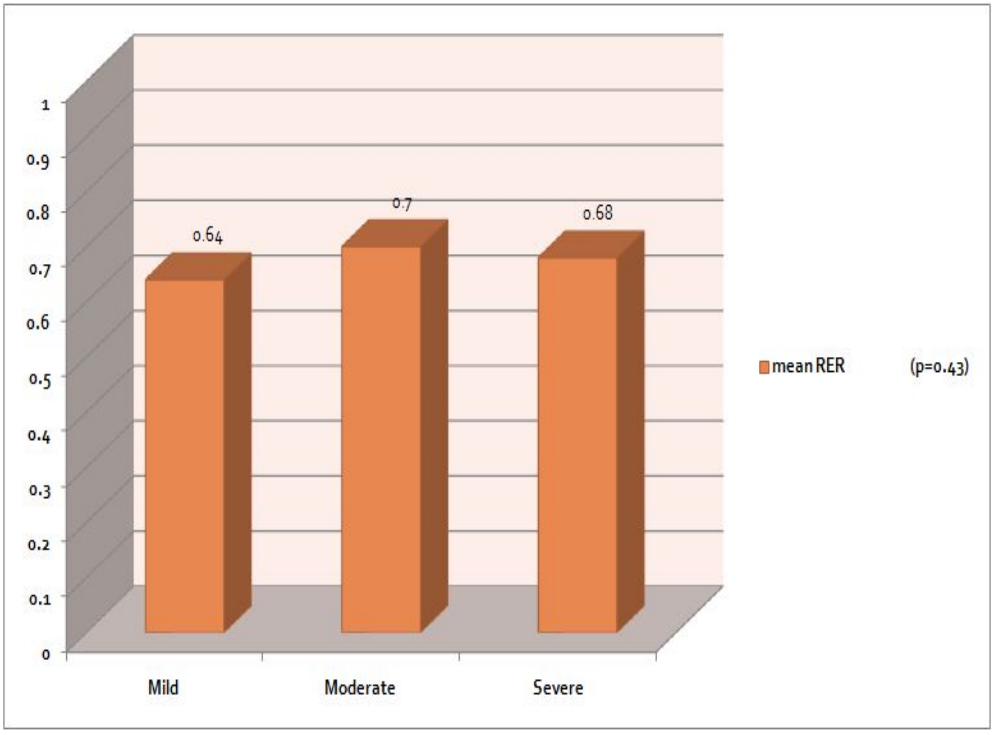

Figure 5. The graphs of relative enhancement ratio (RER) correlation to bile production. There is not statistical correlation between RER and bile production.

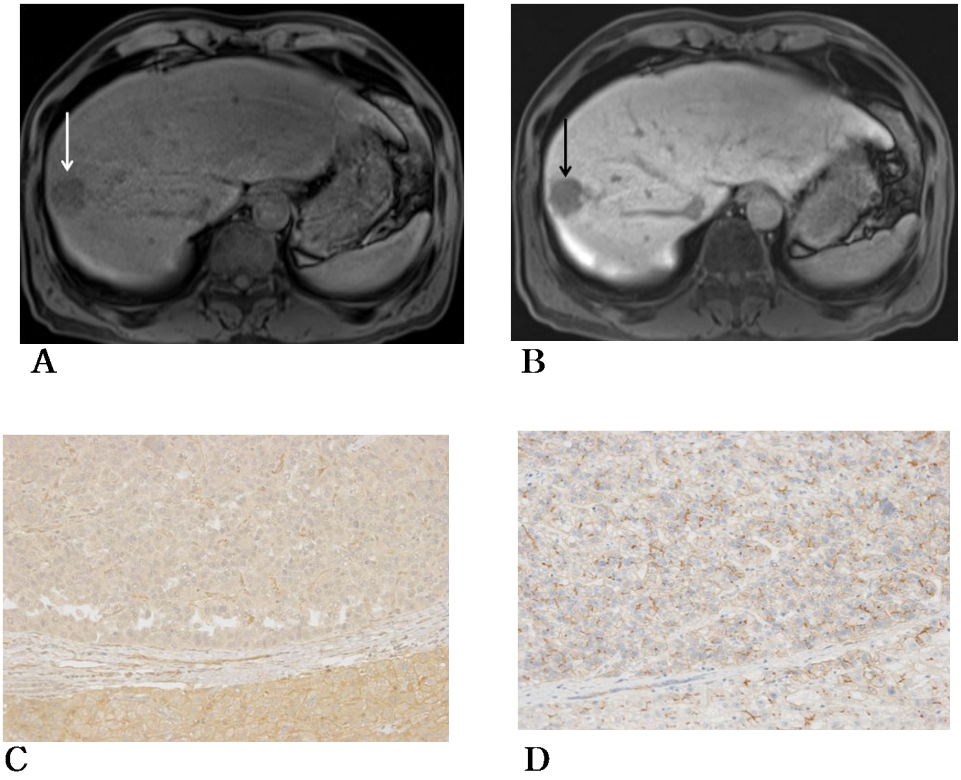

Figure 6. Grade III hepatocellular carcinoma with OATP8 grade 2 and MRP2 grade 1 in 57-year-old man. (A) Pre-contrast MR image shows tumor (white arrow) with the pre-RIR 0.756. (B) Gadoxetic acid-enhanced hepatobiliary phase MR image shows that tumor (black arrow) has the post-RIR 0.61 and the RER 0.807. Immunohistochemical staining (C, D) demonstrated grade 2 (up to 10% and lower than 20% in the extent of the area of the tumor) of OATP8 expression and grade 1 (less than 10% in the extent to the area of the tumor) of MRP2 expression (Original magnification, x 40)

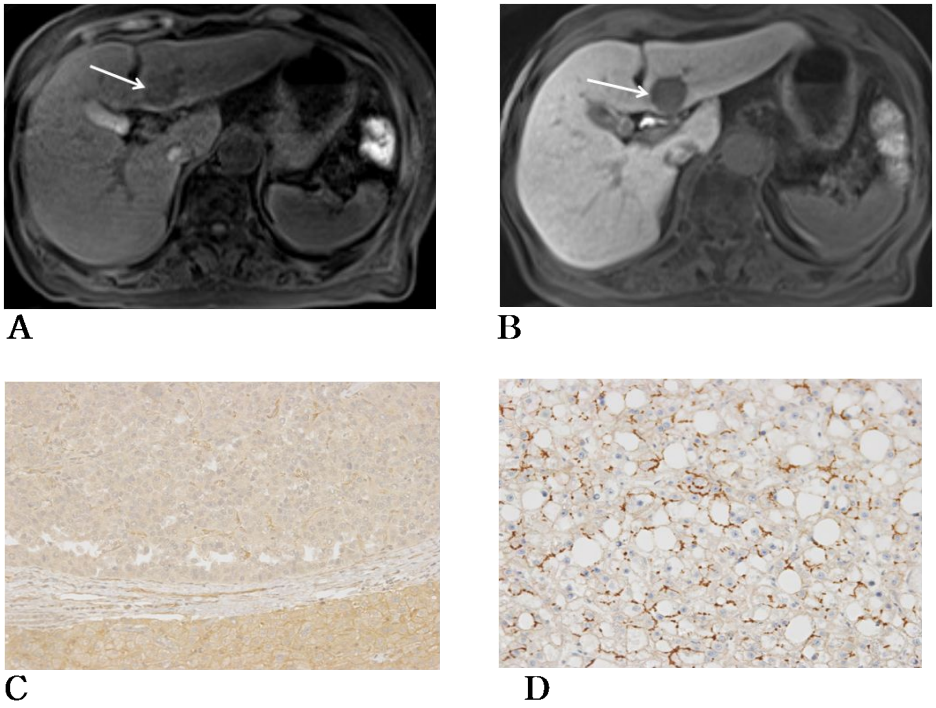

Figure 7. Grade II hepatocellular carcinoma with OATP8 grade 3 and MRP2 grade 3 in 81-year-old female. (A) Pre-contrast MR image showed tumor (arrow, also on b) with the pre-RIR 0.874. (B) Gadoxetic acid-enhanced hepatobiliary phase MR image shows that tumor had the post-RIR 0.466 and the RER 0.534. Immunohistochemical staining (C, D) demonstrated grade 3 (up to 20% in the extent of the area of the tumor) of OATP8 expression and grade 3 (up to 20% in the extent of the area of the tumor) of MRP2 expression The tumor showed increased MRP2 expression at the canalicular membrane (Original magnification, x 100).

IV. Discussion

Gadoxetic acid provides a delayed hepatobiliary imaging as well as a dynamic perfusion imaging because it combines the properties of a conventional extracellular fluid contrast agent and a hepatocyte-specific agent (1-3). On dynamic perfusion MR imaging with gadoxetic acid, HCCs show mostly hyperintense or peripheral hyperintense rim and hypointense tumors during delayed hepatobiliary imaging. There are best tumor delineation on late delayed images taken at 20minutes after gadoxetic acid injection (6). Thus, it improves the detection and characterization of HCCs. The recent study was reported that higher sensitivities and specificities can be achieved with addition of hepatobiliary phase MR imaging, compared with those obtained with routine MR imaging (10, 12). Typically, most HCCs are devoid of hepatocytes so that they appear hypointense tumors against the bright background liver on hepatobiliary phase of gadoxetic acid-enhanced MR imaging (4, 6, 8). However, several studies have been shown paradoxical tumor enhancement in gadoxetic acid-enhanced MR imaging, especially in HCC (23-25). Tumors with hepatocellular elements, such as focal nodular hyperplasia and hepatocellular adenoma, or

those with a relevant blood pool like hemangiomas may show uptake of gadoxetic acid and therefore an increase in signal intensity on hepatobiliary images (4). It is difficult to diagnosis confidently to some HCCs with positive contrast enhancement of gadoxetic acid.

Positive contrast enhancement of HCCs on gadoxetic acid-enhanced hepatobiliary-phase images can be theoretically related to both active uptake of gadoxetic acid by HCCs with a residual hepatocyte function and impaired biliary excretion within the intratumoral region (7, 8, 21, 23). It seems that only highly differentiated HCCs and benign nodules can possibly preserve this hepatocyte function (24-26). Although well- and moderate-differentiated HCCs show to be more enhanced than the surrounding hepatic parenchyma in hepatobiliary phase of gadoxetic acid-enhanced MR imaging, these positive enhancement of HCCs is not definite predictor for the extent of tumor differentiation. In my study, 30 HCCs with grade I and II were shown as all hypointensity tumors on hepatobiliary phase of gadoxetic acid-enhanced MR imaging. The pattern of tumor proliferation scarcely affected gadoxetic acid uptake of the tumor cells.

The post-contrast RSIs were significantly decreased compared with the pre-contrast RSIs in all cases of my study. The

decline of the contrast medium in the tumor blood spaces relatively to the surrounding non-tumorous area and that the tumor cells hardly took up gadoxetic acid due to loss of hepatic function reserves (27). The descent of RSIs of HCCs after administration of gadoxetic acid was not correlated with Edmondson-Steiner grade as well as tumor proliferative pattern.

Bile production is most typically observed in relatively well-differentiated HCCs as compared to poorly differentiated HCCs, especially in moderately differentiated HCCs as compared to well-differentiated HCCs and appear with a green color in resected specimens, so called green hepatoma (15). Kiato et al (17) recently reported iso- or hyperintense HCCs showed pseudoglandular proliferation with bile plugs with significantly high frequency. However, Lee et al (28) showed that most non-hypointense areas of HCCs on gadoxetic acid-enhanced hepatobiliary-phase images may be not associated with microscopic difference of bile production, which is similar to a finding of a previous report (21). My result also showed that bile production is not related with tumoral enhancement.

Gadoxetic acid is transported into the tumor cells via OATP8 then accumulated in extracellular cytoplasm. Gadoxetic acid with hyperintense HCC is relatively more accumulated than in surrounding hepatocytes. Recent studies have been shown the

enhancement ratio of HCCs in the hepatobiliary phase of gadoxetic acid-enhanced MR imaging positively correlated with expression levels of OATP8. The degree of OATP8 expression was higher in hyperintense HCCs than in background liver (15, 17). However, background expression score of OATP8 was higher than tumor expression score in my study. The low expression activity of OATP8 in HCCs to surrounding adjacent liver parenchyma might assume responsibility for HCCs with hypointensity.

MRP2, which is well known a major export transporter on the canalicular side, was constantly expressed in hypointense and hyperintense HCCs (16, 18). It means that the excretion of gadoxetic acid from HCC cells into the tumor sinusoids is enhanced, probably because of the depletion of bile ducts in HCCs. In my study, the expression of MRP2 in tumor cells was higher than that in surrounding liver. There was no HCCs with hyperintensity on hepatobiliary phase images of gadoxetic acid-enhanced MR imaging. The higher MRP2 expression degree was shown the lower tumor RER in HCC cells. Thus, up-regulation of MRP2 in HCCs may cause the highly activated excretion of gadoxetic acid into bile canaliculi , and the it may result in the drop of signal intensity.

My study had some limitations. First, my study could not avoid

sampling bias because of its retrospective design. Second, my study did not include HCCs with high signal intensity. Therefore, I couldn't evaluate whether the expression activity of OATP8 is affected in gadoxetic acid uptake to HCCs with high signal intensity. Third, I didn't consider the role of MRP3 in gadoxetic acid uptake in HCC cells. The interaction between OATP8, MRP2 and MRP3 should be further studied for making clear mechanism of gadoxetic acid uptake in HCCs. In addition, there are many other transporters expressed at the membrane of hepatocytes (29). However, I did not exclude these factors that might affect accumulation or excretion of gadoxetic acid in HCC cells.

In conclusion, gadoxetic acid uptake on hepatobiliary phases MR imaging is not determined by tumor differentiation, proliferation or bile production of HCC. The gadoxetic acid-enhancement of HCC is directly influenced by up-regulation of MRP2 rather than the expression activity of OATP8.

SUMMARY

The purpose of this study is to evaluate the mechanism of gadoxetic acid uptake of hepatocellular carcinoma (HCC) on hepatobiliary phase of gadoxetic acid-enhanced magnetic resonance (MR) imaging and to correlate the enhancement of HCCs with histopathologic features and molecular transporters. Forty HCC nodules with surgical confirmation had undergone dynamic MRI. T1-weighted 3D gradient echo sequences before and 20 min (hepatobiliary phase) after the injection of gadoxetic acid were performed. To assess gadoxetic acid uptake, the relative enhancement ratio (RER) of tumor was calculated with the relative signal intensity (RSI) ratio of tumor to adjacent hepatic parenchyma. The Edmondson-Steiner grading (I-IV), presence of tumor capsule, proliferation pattern (trabecular, pseudoglandular, compact), and the degree of bile production (mild, moderate, severe) were reviewed. The expression degree of OATP8 and MRP2 in the tumors was assessed (three grades, respectively) by the immunohitochemical staining. Mean RER of the tumor was 0.65±0.11. RERs of Edmondson-Steiner grade I , grade II and grade III HCCs were 0.72±0.11, 0.63±0.23, and 0.68±0.10, respectively (P=0.32). RERs of HCCs with trabecular,

pseudoglandular, and compact pattern were 0.69±0.12, 0.62±0.01, and 0.62±0.09 (P=0.26). RERs of HCCs with mild, moderate, and severe bile production were 0.64±0.01, 0.70±0.11, and 0.68±0.10, respectively (P=0.43). The correlation coefficient (r) of expression degree of OATP8 and MRP2 in the tumors was 0.055 (P=0.735) and -0.325 (P=0.038), respectively. The tumor enhancement ratio was strong negatively correlated to the expression degree of MRP2. These results suggest that gadoxetic acid uptake on hepatobiliary phase MR imaging is not determined by tumor differentiation, proliferation or bile production of HCC. The gadoxetic acid-enhancement of HCC is directly influenced by up-regulation of MRP2 rather than the expression activity of OATP8.

REFERENCES

1. Reimer P, Schneider G, Schima W. Hepatobiliary contrast agents for contrast-enhanced MRI of the liver: properties, clinical development and applications. *Eur Radiol* 2004; 14:559 - 578.
2. Balci NC, Semelka RC. Contrast agents for MR imaging of the liver. *Radiol Clin North Am* 2005;43:887 - 898.
3. Seale MK, Catalano OA, Saini S, Hahn PF, Sahani DV. Hepatobiliary-specific MR contrast agents: role in Imaging the liver and biliary tree. *RadioGraphics* 2009; 29:1725 - 1748.
4. Hamm B, Staks T, Muhler A, et al. Phase I clinical evaluation of Gd-EOB-DTPA as a hepatobiliary MR contrast agent: safety, pharmacokinetics, and MR imaging. *Radiology* 1995; 195:785-792.
5. Reimer P, Rummeny EJ, Shamsi K, et al. Phase II clinical evaluation of Gd-EOB-DTPA: dose, safety aspects, and pulse sequence. *Radiology* 1996; 199:177-183.
6. Frericks BB, Loddenkemper C, Huppertz A, et al. Qualitative and quantitative evaluation of hepatocellular carcinoma and cirrhotic liver enhancement using Gd-EOB-DTPA.

AJR 2009; 193:1053-1060.

7. Vogl TJ, Kummel S, Hammerstingl R, et al. Liver tumors: comparison of MR imaging with Gd-EOB-DTPA and Gd-DTPA. *Radiology* 1996; 200:59-67.
8. Sun HY, Lee JM, Shin CI, et al. Gadoxetic acid-enhanced magnetic resonance imaging for differentiating small hepatocellular carcinomas (< or =2 cm in diameter) from arterial enhancing pseudolesions: special emphasis on hepatobiliary phase imaging. *Invest Radiol* 2010; 45:96-103.
9. Huppertz A, Haraida S, Kraus A, et al. Enhancement of Focal Liver Lesions at Gadoxetic Acid - enhanced MR imaging: correlation with histopathologic findings and spiral CT— initial observations1. *Radiology* 2005; 234:468-478
10. Hammerstingl R, Huppertz A, Breuer J, et al. Diagnostic efficacy of gadoxetic acid (Primovist)-enhanced MRI and spiral CT for a therapeutic strategy: comparison with intraoperative and histopathologic findings in focal liver lesions. *Eur Radiol* 2008; 18:457-467.
11. Filippone A, Blakeborough A, Breuer J, et al. Enhancement of liver parenchyma after injection of hepatocyte-specific MRI contrast media: a comparison of gadoxetic acid and gadobenate dimeglumine. *J Magn Reson Imaging* 2010;

31:356-64.

12. Ahn SS, Kim MJ, Lim JS, et al. Added value of gadoxetic acid-enhanced hepatobiliary phase MR imaging in the diagnosis of hepatocellular carcinoma. *Radiology* 2010; 255:459-466.
13. Leonhardt M, Keiser M, Oswald S, et al. Hepatic uptake of the magnetic resonance imaging contrast agent Gd-EOB-DTPA: role of human organic anion transporters. *Drug Metab Dispos* 2010; 38:1024-1028.
14. Schuhmann-Giampieri G, Schmitt-Willich H, Press WR, et al. Preclinical evaluation of Gd-EOB-DTPA as a contrast agent in MR imaging of the hepatobiliary system. *Radiology* 1992; 183:59-64.
15. Narita M, Hatano E, Arizono S, et al. Expression of OATP1B3 determines uptake of Gd-EOB-DTPA in hepatocellular carcinoma. *J Gastroenterol* 2009; 44:793-798.
16. Tsuboyama T, Onishi H, Kim T, et al. Hepatocellular carcinoma: hepatocyte-selective enhancement at gadoxetic acid - enhanced MR imaging—correlation with expression of sinusoidal and canalicular transporters and bile accumulation. *Radiology* 2010; 255:824-833.
17. Kiato A, Zen Y, Mastui O, et al. Hepatocellular carcinoma: signal intensity at gadoxetic acid-enhanced MR Imaging;

correlation with molecular transporters and histopathologic features. *Radiology* 2010; 256:817-826.

18. Tsuda N, Matsui O. Cirrhotic rat liver: reference to transporter activity and morphologic changes in bile canaliculi-gadoxetic acid-enhanced MR imaging. *Radiology* 2010; 256:767-773.
19. Pastoer CM. Fadoxetic acid-enhanced hepatobiliary phase MR imaging: cellular insight. *Radiology* 2010; 257:589-596.
20. Ni Y, Chen F, Wang H, et al. Proper definition of MRI contrast enhancement in liver tumors. *J Gastroenterol* 2010; 45:349-350.
21. Edmondson HA, Steiner PE. Primary carcinoma of the liver: a study of 100 cases among 48,900 necropsies. *Cancer* 1954; 7:462-503.
22. Ruby SG. Protocol for the examination of specimens from patients with hepatocellular carcinoma and cholangiocarcinoma, including intrahepatic bile ducts: a basis for checklists. *Arch Pathol Lab Med* 2000; 124:41-45.
23. Ni, Y, Marchal G, Yu J, et al. Prolonged positive contrast enhancement with Gd-EOB-DTPA in experimental liver tumors: potential value in tissue characterization. *J Magn Reson Imaging* 1994; 4:355-363.

24. Fujita M, Yamamoto R, Takahashi M, et al. Paradoxic uptake of Gd-EOB-DTPA by hepatocellular carcinoma in mice: quantitative image analysis. *J Magn Reson Imaging* 1997; 7:768-770
25. Saito K, Kotake F, Ito N, et al. Gd-EOB-DTPA enhanced MRI for hepatocellular carcinoma: quantitative evaluation of tumor enhancement in hepatobiliary phase. *Magn Reson Med Sci* 2005; 4:1-9.
26. Kogita S, Imai Y, Okada M, et al. Gd-EOB-DTPA-enhanced magnetic resonance images of hepatocellular carcinoma: correlation with histological grading and portal blood flow. *Eur Radiol* 2010; 20:2405-2413.
27. Tajima T, Takao H, Akai H, et al. Relationship between liver function and liver signal intensity in hepatobiliary phase of gadolinium ethoxybenzyl diethylenetriamine pentaacetic acid-enhanced magnetic resonance imaging. *J Comput Assist Tomogr* 2010;34:362-366.
28. Lee SH, Kim SH, Park CK, et al. Comparison between areas with Gd-EOB-DTPA uptake and without in hepatocellular carcinomas on Gd-EOB-DTPA-enhanced hepatobiliary phase MR imaging: pathological correlation. *J Magn Reson Imaging* 2010; 32:719-725.
29. Pauli-Magnus C, Meier PJ. Hepatobiliary transporters and

drug-induced cholestasis. *Hepatology* 2006; 44:778-787.

저작물 이용 허락서

학 과	의	학 번	20087419	과 정	박사
성 명	한글: 최 수 진	한문: 崔 수 珍		영문: Soo Jin Choi	
주 소	경기도 고양시 일산 서구 문촌마을 19단지 신우아파트 1909-603				
연락처	E-mail : drchoi126@hanmail.net				
논문제목	한글: 간세포암의 gadoxetic acid 섭취: 조직학적 성상과 분자 운반체와의 상관관계				
	영문: Gadoxetic acid uptake of hepatocellular carcinoma: Correlation with pathologic features and molecular transporters				

본인이 저작한 위의 저작물에 대하여 다음과 같은 조건 아래 조선대학교가 저작물을 이용할 수 있도록 허락하고 동의합니다.

- 다 음 -

1. 저작물의 DB구축 및 인터넷을 포함한 정보통신망에의 공개를 위한 저작물의 복제, 기억장치에의 저장, 전송 등을 허락함.
2. 위의 목적을 위하여 필요한 범위 내에서의 편집과 형식상의 변경을 허락함. 다만, 저작물의 내용변경은 금지함.
3. 배포·전송된 저작물의 영리적 목적을 위한 복제, 저장, 전송 등은 금지함.
4. 저작물에 대한 이용기간은 5년으로 하고, 기간종료 3개월 이내에 별도의 의사 표시가 없을 경우에는 저작물의 이용기간을 계속 연장함.
5. 해당 저작물의 저작권을 타인에게 양도하거나 출판을 허락을 하였을 경우에는 1개월 이내에 대학에 이를 통보함.
6. 조선대학교는 저작물 이용의 허락 이후 해당 저작물로 인하여 발생하는 타인에 의한 권리 침해에 대하여 일체의 법적 책임을 지지 않음.
7. 소속 대학의 협정기관에 저작물의 제공 및 인터넷 등 정보통신망을 이용한 저작물의 전송·출력을 허락함.

동의여부 : 동의(0) 반대( )

2011 년 8 월 일

저작자: 최 수 진 (인)

조선대학교 총장 귀하